

**MACHINE VISION APPLICATION FOR AUTOMATIC DEFECT  
SEGMENTATION IN WELD RADIOGRAPHS**

**by**

**SOO SAY LEONG**

**Thesis submitted in fulfillment of the requirements  
for the degree of  
Master of Science**

**April 2006**

## ACKNOWLEDGEMENTS

First of all, I would like to take this opportunity to thank my supervisors, Dr. Zahurin Samad and Associate Professor Dr. Mani Maran for their support, motivation and inspirational supervising through out the research and thesis writing process. In many stages of the research, their profound expertise and professional knowledge provided key injection to the technical solutions. Without their effort and guidance, this research would never have been completed. I also wish to express my sincere thanks to Mr. Lim Teong Yeong, for his unlimited support through out the research.

Great thanks to my beloved parents for their immeasurable support, patient and understanding. Without them, I could not have been able to complete my studies here. To all my brothers and sister, thank you for being there always.

Last but not least, my sincere thanks to the School of Mechanical Engineering, University Science of Malaysia and the Ministry of Science, Technology and Environment (Malaysia) for the offer of the IRPA that enabled this work to be carried out.

## **CHAPTER THREE : AUTOMATIC LABEL REMOVAL FROM DIGITIZED WELD RADIOGRAPHS**

|       |                                      |    |
|-------|--------------------------------------|----|
| 3.1   | Introduction                         | 31 |
| 3.2   | Weld radiographic image digitization | 31 |
| 3.3   | Labels on weld radiograph            | 32 |
| 3.4   | Label removal                        | 34 |
| 3.4.1 | Contrast enhancement                 | 35 |
| 3.4.2 | Intensity profile normality test     | 37 |
| 3.4.3 | Label pixels detection               | 49 |
| 3.4.4 | Label region merging                 | 54 |
| 3.4.5 | Label region removal                 | 57 |
| 3.5   | Results and discussions              | 60 |
| 3.6   | Summary                              | 63 |

## **CHAPTER FOUR : WELD EXTRACTION BY GRAPHICAL ANALYSIS ON WELD INTENSITY PROFILE**

|       |  |    |
|-------|--|----|
| 4.1   | Introduction   | 65 |
| 4.2   | Background study   | 65 |
| 4.3   | Weld extraction  | 66 |
| 4.3.1 | Intensity profile of weld radiographic images                      | 66 |
| 4.3.2 | Weld boundary points detection on approximated<br>Gaussian profile | 68 |
| 4.3.3 | Noise removal  | 74 |
| 4.3.4 | Weld boundary points detection on radiograph<br>intensity profile  | 77 |
| 4.3.5 | Weld area extraction   | 82 |
| 4.4   | Results and discussions  | 84 |
| 4.4   | Summary  | 87 |

## **CHAPTER FIVE : AUTOMATIC WELD DEFECT SEGMENTATION USING RANK LEVELING TECHNIQUE**

|        |   |     |
|--------|---|-----|
| 5.1    | Introduction  | 89  |
| 5.2    | Background study  | 89  |
| 5.3    | Defect segmentation                                       | 90  |
| 5.3.1  | Region of interest selection                              | 91  |
| 5.3.2  | Background subtraction method                             | 92  |
| 5.3.3  | Rank leveling   | 93  |
| 5.3.4  | Filtered profile correction                               | 95  |
| 5.3.5  | Selection of rank filter size                             | 98  |
| 5.3.6  | Background estimation and subtraction by rank<br>leveling | 100 |
| 5.3.7  | Comparative study on background estimation methods        | 100 |
| 5.3.8  | Contrast enhancement of leveled image                     | 105 |
| 5.3.9  | Image binarization  | 109 |
| 5.3.10 | Post-processing by morphological reconstruction           | 111 |
| 5.4    | Results and discussions                                   | 113 |
| 5.4    | Summary   | 116 |

## **CHAPTER SIX : INTEGRATION OF LABEL REMOVAL, WELD EXTRACTION AND DEFECT SEGMENTATION ALGORITHMS**

|     |                        |     |
|-----|------------------------|-----|
| 6.1 | Introduction           | 118 |
| 6.2 | Algorithms integration | 118 |
| 6.3 | Result and discussions | 123 |
| 6.4 | Summary                | 124 |

## **CHAPTER SEVEN : CONCLUSIONS AND FUTURE RESEARCH**

|     |                                     |     |
|-----|-------------------------------------|-----|
| 7.1 | Conclusion                          | 125 |
| 7.2 | Contributions of the research       | 126 |
| 7.2 | Recommendations for future research | 127 |

|  |     |
|--|-----|
| <b>REFERENCES</b>  | 128 |
| <br>   |     |
| <b>APPENDICES</b>  |     |
| Appendix A : Normal curve area   | 132 |
| Appendix B : Automatic weld defect segmentation methodology<br>results | 133 |
| B1    Sample image 1 (lack of penetration defect)                      | 133 |
| B2    Sample image 2 (slag inclusion defect)                           | 136 |
| B3    Sample image 3 (lack of penetration defect)                      | 139 |
| B4    Sample image 4 (porosity defect)                                 | 142 |
| B5    Sample image 5 (crack defect)                                    | 145 |
| Appendix C : Pseudo Code for Algorithms Developed                      | 148 |
| C1    Pseudo Code for Label Removal Algorithm                          | 148 |
| C2    Pseudo Code for Weld Extraction Algorithm                        | 150 |
| C3    Pseudo Code for Defect Segmentation Algorithm                    | 151 |
| C4    Pseudo Code for <i>outliers_detection</i> Function               | 152 |
| <br>   |     |
| <b>LIST OF PUBLICATIONS &amp; SEMINARS</b>                             | 153 |

## LIST OF TABLES

|           |   | Page |
|-----------|---|------|
| Table 1.1 | Typical weld defects in weld radiographs  | 2    |
| Table 3.1 | Intensity histogram and calculation of IQR/ <i>stdev</i> ratio.                 | 40   |
| Table 3.2 | Ratio of IQR/ <i>stdev</i> for Type 1 – 4 intensity profile.                    | 41   |
| Table 3.3 | Ratio of IQR/ <i>stdev</i> and R-square value for Type 1 – 4 intensity profile. | 47   |

## LIST OF FIGURES

|                |  | Page |
|----------------|--|------|
| Figure 2.1     | Classification of welding process.                             | 11   |
| Figure 2.2     | Three distinct zones of a typical arc welding joint.           | 12   |
| Figure 2.3     | Radiographic testing.  | 14   |
| Figure 2.4(a)  | Typical radiographic image.                                    | 17   |
| Figure 2.4(b)  | Image from manual interpretation of the weld.                  | 17   |
| Figure 2.4(c)  | Template image used to train neural network.                   | 17   |
| Figure 2.5(a)  | Gaussian-like intensity profile.                               | 19   |
| Figure 2.5(b)  | Non-Gaussian intensity profile.                                | 19   |
| Figure 2.6(a)  | Peak anomaly.  | 21   |
| Figure 2.6(b)  | Trough anomaly.  | 21   |
| Figure 2.6(c)  | Slant-concave-anomaly.   | 21   |
| Figure 2.7(a)  | Laws filter.   | 23   |
| Figure 2.7(b)  | Kirsch filter.   | 23   |
| Figure 2.8(a)  | ANN neural network architecture for edge detection.            | 25   |
| Figure 2.8(b)  | Some cases for contour used as training couples of ANN.        | 26   |
| Figure 2.9(a)  | Inclusion defect.  | 26   |
| Figure 2.9(b)  | Crack defect.  | 26   |
| Figure 2.10(a) | Summary of literature review on automatic weld extraction.     | 29   |
| Figure 2.10(b) | Summary of literature review on automatic defect segmentation. | 29   |
| Figure 3.1     | Example of a reference radiograph of IIW.                      | 32   |
| Figure 3.2(a)  | Hole-type IQI.   | 33   |
| Figure 3.2(b)  | Wire-type IQI.   | 33   |
| Figure 3.3     | Labels on weld radiograph.                                     | 33   |
| Figure 3.4     | Labels removal methodology.                                    | 34   |

|                 |   |    |
|-----------------|---|----|
| Figure 3.5      | Linear image mapping.   | 35 |
| Figure 3.6(a)   | Original image before contrast enhancement.   | 36 |
| Figure 3.6(b)   | Image after contrast enhancement.   | 36 |
| Figure 3.7(a)   | Image histogram before contrast stretching.   | 36 |
| Figure 3.7(b)   | Image histogram after contrast stretching.  | 36 |
| Figure 3.8      | 4 types of intensity profile taken in $i$ - direction.                                | 37 |
| Figure 3.9      | IQR for a standard normal distribution.   | 39 |
| Figure 3.10     | Plot of IQR/ <i>stdev</i> ratio for Type 1 – 4 intensity profile.                     | 42 |
| Figure 3.11     | Weld radiograph with large labels.  | 43 |
| Figure 3.12     | Intensity histogram for pixels along $j = 30$ .                                       | 43 |
| Figure 3.13     | Normal probability plot for pixels along $j = 30$ .                                   | 45 |
| Figure 3.14     | Plot of normal probability plot R-square value for Type 1 – Type 4 intensity profile. | 48 |
| Figure 3.15     | Intensity profile normality test operation.   | 49 |
| Figure 3.16     | Intensity profile taken across labels on $j = 223$ .                                  | 50 |
| Figure 3.17     | Intensity histogram of intensity profile on $j = 223$ .                               | 51 |
| Figure 3.18     | Example 1 – label pixel detection.  | 53 |
| Figure 3.19     | Example 2 – label pixel detection.  | 54 |
| Figure 3.20     | Dilation result with different size of structuring element.                           | 56 |
| Figure 3.21     | Merging of labels region for image shown in Figure 3.18.                              | 56 |
| Figure 3.22     | Merging of labels region for image shown in Figure 3.19.                              | 57 |
| Figure 3.23     | Example of Feret boxes.   | 57 |
| Figure 3.24 (a) | Constructed Feret boxes for label regions.  | 58 |
| Figure 3.24(b)  | Removal of label pixels which located inside Feret boxes.                             | 58 |
| Figure 3.25(a)  | Image 3D plot before label removal.   | 59 |
| Figure 3.25(b)  | Image 3D plot after label removal.  | 59 |

|                |  |    |
|----------------|--|----|
| Figure 3.26    | Results of label removal algorithm.  | 60 |
| Figure 3.27(a) | Weld radiograph with large labels.   | 61 |
| Figure 3.27(b) | Labels remain after the application of label removal algorithm with IQR/ <i>stdev</i> ratio technique.                             | 61 |
| Figure 3.27(c) | Labels successfully removed with the combination of IQR/ <i>stdev</i> ratio and normal probability plot R-square value techniques. | 61 |
| Figure 3.28    | Results of label removal algorithm – example 1.  | 62 |
| Figure 3.29    | Results of label removal algorithm – example 2.  | 62 |
| Figure 3.30    | Results of label removal algorithm – example 3.  | 63 |
| Figure 4.1     | Weld radiographic image.   | 65 |
| Figure 4.2     | Intensity profile of weld radiographic image.  | 67 |
| Figure 4.3     | Intensity profile after normalization operation.   | 69 |
| Figure 4.4     | Approximated Gaussian distribution curve.  | 69 |
| Figure 4.5     | Weld boundary point location.  | 69 |
| Figure 4.6     | Gaussian Plot, straight line and distance plot.  | 70 |
| Figure 4.7     | Weld boundary point detection on approximated Gaussian Curve.  | 74 |
| Figure 4.8(a)  | Original intensity profile.  | 76 |
| Figure 4.8(b)  | Intensity profile for image smoothing by $3 \times 1$ filter mask.   | 76 |
| Figure 4.8(c)  | Intensity profile for image smoothing by $7 \times 1$ filter mask.   | 76 |
| Figure 4.8(d)  | Intensity profile for image smoothing by $9 \times 1$ filter mask.   | 76 |
| Figure 4.9     | Weld boundary point detection on intensity profile.  | 77 |
| Figure 4.10(a) | Image of a crack defect.   | 78 |
| Figure 4.10(b) | Intensity profile taken across crack defect.   | 78 |
| Figure 4.11(a) | Detection of false peak.   | 79 |
| Figure 4.11(b) | Actual and detected boundary points.   | 79 |

|                |  |     |
|----------------|--|-----|
| Figure 4.12    | Weld boundary points detection on intensity profile taken across crack defect with modified algorithm. | 81  |
| Figure 4.13    | Weld boundary points detection on intensity profile taken across good weld with modified algorithm.    | 81  |
| Figure 4.14(a) | A 224 x 573 pixels weld radiograph.  | 82  |
| Figure 4.14(b) | Extracted weld.  | 82  |
| Figure 4.15(a) | False detection of weld boundary points.   | 84  |
| Figure 4.15(b) | Extracted weld after removing false detection.   | 84  |
| Figure 4.16    | Weld extractions on weld radiograph with Gaussian-like and non-Gaussian intensity profile.             | 85  |
| Figure 4.17    | Various weld radiographs with detected weld boundary.  | 87  |
| Figure 4.18    | Weld extraction methodology.   | 88  |
| Figure 5.1     | Label removal, weld extraction and defect segmentation algorithm.                                      | 91  |
| Figure 5.2(a)  | Detected weld boundaries.  | 92  |
| Figure 5.2(b)  | Cropped ROI – weld region.   | 92  |
| Figure 5.3(a)  | Original image intensity profile.  | 93  |
| Figure 5.3(b)  | Estimated background profile.  | 93  |
| Figure 5.3(c)  | Detected defect area profile.  | 93  |
| Figure 5.4     | Illustration of the working principle of rank value filters with a $3 \times 1$ maximum filters.       | 94  |
| Figure 5.5     | Application maximum rank filter on a defective intensity profile.                                      | 95  |
| Figure 5.6     | Spreading effect of filtered profile.  | 96  |
| Figure 5.7     | Corrected-filtered profile.  | 97  |
| Figure 5.8     | Corrected-filtered profile and the result of BSM.  | 98  |
| Figure 5.9     | Rank filtering of corrected-filtered profile by an undersize window.                                   | 99  |
| Figure 5.10(a) | Original image.  | 100 |
| Figure 5.10(b) | Estimated background image by rank leveling technique with filtered-profile correction.                | 100 |

|                |   |     |
|----------------|---|-----|
| Figure 5.10(c) | Leveled image with suspected defects.   | 100 |
| Figure 5.11(a) | Original image.   | 101 |
| Figure 5.11(b) | Estimated background image by surface fitting algorithm with polynomial function.   | 101 |
| Figure 5.11(c) | Leveled image with suspected defects.   | 101 |
| Figure 5.12    | Weld radiograph with uniformly illuminated background.  | 102 |
| Figure 5.13    | Weld radiograph with non-uniformly illuminated background.  | 102 |
| Figure 5.14    | Comparison of BSM by rank leveling technique and polynomial surface fitting algorithm on uniformly illuminated background radiograph.     | 103 |
| Figure 5.15    | Comparison of BSM by rank leveling technique and polynomial surface fitting algorithm on non-uniformly illuminated background radiograph. | 104 |
| Figure 5.16    | Contrast stretching on leveled image shown in Figure 5.14(b).   | 105 |
| Figure 5.17    | Leveled Image histogram before and after contrast stretching.   | 106 |
| Figure 5.18    | Heavily contaminated leveled image after contrast stretching.   | 106 |
| Figure 5.19    | Intensity profile taken across <i>a-a</i> in Figure 5.18.   | 107 |
| Figure 5.20    | Result of gamma correction with gamma value = 0.5 on image shown in Figure 18.  | 108 |
| Figure 5.21    | Result of gamma correction with gamma value = 2 on image shown in Figure 18.  | 108 |
| Figure 5.22    | Intensity profile – after gamma correction.   | 109 |
| Figure 5.23    | Histogram for image shown in Figure 5.21.   | 110 |
| Figure 5.24    | Thresholding result on image after gamma correction as shown in Figure 5.21.  | 110 |
| Figure 5.25    | Thresholding result on image before gamma correction as shown in Figure 5.18.   | 111 |
| Figure 5.26    | Post-processing operation by morphological reconstruction.  | 112 |
| Figure 5.27    | Post-processed of image shown in Figure 5.24.   | 112 |

|               |   |     |
|---------------|---|-----|
| Figure 5.28   | Example 1 of defect detection on defective weld radiograph.   | 113 |
| Figure 5.29   | Example 2 of defect detection on defective weld radiograph.   | 114 |
| Figure 5.30   | Example 3 of defect detection on defective weld radiograph.   | 114 |
| Figure 5.31   | Example of defect detection on defect free weld radiograph.   | 114 |
| Figure 5.32   | Tungsten inclusion defect was unable to be detected by defect detection methodology developed in this research. | 115 |
| Figure 6.1    | Integration of Label removal, Weld extraction and Defect segmentation algorithms.                               | 119 |
| Figure 6.2(a) | Original input image.   | 120 |
| Figure 6.2(b) | Contrast enhanced image after contrast enhancement.   | 120 |
| Figure 6.2(c) | Label-free image after the application of label removal algorithm.  | 120 |
| Figure 6.3(a) | Image after noise removal.  | 121 |
| Figure 6.3(b) | Image showing detected weld boundaries.   | 121 |
| Figure 6.4(a) | Cropped ROI image.  | 123 |
| Figure 6.4(b) | Estimated background image by using rank leveling technique.  | 123 |
| Figure 6.4(c) | Leveled image by using background subtraction method.   | 123 |
| Figure 6.4(d) | Leveled image after contrast stretching and gamma correction.   | 123 |
| Figure 6.4(e) | Binarized image.  | 123 |
| Figure 6.4(f) | Output image after post-processing.   | 123 |

## LIST OF SYMBOLS

|              |   |
|--------------|---|
| $m$          | Filter window row numbers   |
| $n$          | Filter window column numbers  |
| $i$          | Horizontal axis of weld radiograph                                      |
| $j$          | Vertical axis of weld radiograph  |
| $A$          | Corresponding tail area of the standard normal ( $z$ ) distribution     |
| $E$          | Estimated expected value under normality                                |
| $r^2$        | R-square value or coefficient of determination                          |
| $L$          | Total gray levels of an image   |
| $n_r$        | The number of pixels at level $r$                                       |
| $p_r$        | The probability of $r$ gray level in an image                           |
| $N$          | Total number of pixels in an image                                      |
| $\mu_1$      | Mean value for class 1 of pixels  |
| $\mu_2$      | Mean value for class 2 of pixels  |
| $\mu_T$      | Total mean value for pixels in an image                                 |
| $\sigma_B^2$ | Between class variance  |
| $t^*$        | Optimal threshold value   |
| $\mu$        | Mean of the Gaussian distribution plot                                  |
| $\sigma$     | Standard deviation of the Gaussian distribution plot                    |
| $x$          | Pixel number along $j$ -direction of an image                           |
| $y$          | Intensity value of the pixel along an intensity profile                 |
| $m$          | Gradient of a straight line   |
| $c$          | Interception of the straight line on the $y$ -axis of intensity profile |
| $f$          | A function  |

|           |   |
|-----------|---|
| $h$       | Mask filter   |
| $x_{ctr}$ | Center of spreading   |
| $x_p$     | Pixel located at $p$ along $x$ – axis of an intensity profile |
| $N_p$     | Total numbers of pixel in an intensity profile                |
| $p$       | Location of pixel along an intensity profile                  |
| $D$       | Spreading distance  |
| $q$       | Row size of the rank filter                                   |
| $I_{in}$  | Intensity value of an input image                             |
| $I_{out}$ | Intensity value of an output image                            |
| $G$       | Gamma value   |
| $r$       | Grey level  |

## LIST OF ABBREVIATION

|           |   |
|-----------|---|
| NDT       | Non-destructive testing                               |
| CCD       | Charge coupled device                                 |
| MLP       | Multilayer Perceptron                                 |
| KNN       | K-nearest neighbor                                    |
| MSE       | Mean square error                                     |
| SPSS      | Statistical Package for the Social Sciences           |
| MGED      | Mean gradient edge detector                           |
| AI        | Artificial intelligence                               |
| ANN       | Artificial neural network                             |
| GWIMV     | Gaussian weighted image moment vector operator        |
| FFT       | Fast Fourier transforms                               |
| IIW       | International Institute of Welding                    |
| dpi       | Dots per inch   |
| TIFF      | Tagged image file format                              |
| IQI       | Image quality indicators                              |
| IQR       | Inter-quartile range                                  |
| stdev     | Standard deviation                                    |
| $Q_U$     | Upper quartile  |
| $Q_L$     | Lower quartile  |
| $SS_{yy}$ | Sum of squares of deviation                           |
| SSE       | Sum of squares of error                               |
| FWHM      | Full width value at half maximum of intensity profile |
| ROI       | Region of interest                                    |
| BSM       | Background subtraction method                         |
| blob      | Binary large object                                   |

# **APLIKASI PENGLIHATAN MESIN UNTUK PERUASAN KECACATAN DALAM RADIOGRAF KIMPALAN SECARA AUTOMATIK**

## **ABSTRAK**

Objektif penyelidikan ini adalah untuk membangunkan satu kaedah peruasan kecacatan kimpalan automatik yang boleh meruas pelbagai jenis kecacatan kimpalan yang wujud dalam imej radiografi kimpalan. Kaedah segmentasi kecacatan automatik yang dibangunkan terdiri daripada tiga algoritma utama, iaitu algoritma penyingkiran label, algoritma pengenalpastian bahagian kimpalan dan algoritma segmentasi kecacatan kimpalan. Algoritma penyingkiran label dibangunkan untuk mengenalpasti dan menyingkirkan label yang terdapat pada imej radiograf kimpalan secara automatik, sebelum algoritma pengenalpastian bahagian kimpalan dan algoritma segmentasi kecacatan diaplikasikan ke atas imej radiografi. Satu algoritma pengenalpastian bahagian kimpalan juga dibangunkan dengan tujuan mengenalpasti bahagian kimpalan dalam imej radiograf secara automatik dengan menggunakan profil keamatan yang diperolehi daripada imej radiografi. Algoritma ini mampu mengenalpasti bahagian kimpalan dalam imej radiografi tanpa mengira sama ada profil keamatan yang diperolehi itu mempunyai sifat profil Gaussian atau pun tidak. Akhirnya, algoritma segmentasi kecacatan kimpalan telah dibangunkan untuk mensegmen kecacatan kimpalan secara automatik daripada imej dengan menggunakan teknik penolakan latar belakang dan teknik penyama-rataan secara aturan. Kajian perbandingan antara teknik penyama-rataan secara aturan dan teknik pemadanan permukaan dengan fungsi polinomial juga dilakukan. Adalah didapati bahawa teknik penyama-rataan secara aturan memberikan keputusan yang lebih baik berbanding dengan teknik pemadanan permukaan dengan fungsi polinomial dalam meramal latar belakang untuk imej radiograf kimpalan dalam penyelidikan ini. Kaedah peruasan kecacatan kimpalan automatik yang telah dibangunkan dalam penyelidikan ini telah diuji dengan berjaya

ke atas 30 imej. Penyumbangan penyelidikan ini ialah pembangunan algoritma penyinkiran label secara automatic di mana pada masa kini, masih belum ada penerbitan tentang kajian dalam bidang penyikaran label secara automatik untuk imej radiografi kimpalan yang diterbitkan. Selain itu, algoritma pengenalpastian bahagian kimpalan yang dibangunkan telah membaiki kaedah pengenalpastian bahagian kimpalan Liao dan Ni (1996) yang mana hanya terhad kepada imej radiografi yang mempunyai profil keamatan yang menyerupai bentuk profil Gaussian. Akhirnya, algoritma peruasan kecacatan kimpalan yang telah dibangunkan untuk mensegmen kecacatan kimpalan secara automatic telah dibuktikan dapat meruas kecacatan dalam imej yang mengandungi hingar dan pencerahan tidak serata.

# **MACHINE VISION APPLICATION FOR AN AUTOMATIC DEFECT**

## **SEGMENTATION IN WELD RADIOGRAPHS**

### **ABSTRACT**

The objective of the research is to develop an automatic weld defect segmentation methodology to segment different types of defects in radiographic images of welds. The segmentation methodology consists of three main algorithms, namely label removal algorithm, weld extraction algorithm and defect segmentation algorithm. The label removal algorithm was developed to detect and remove labels that are printed on weld radiographs automatically before weld extraction algorithm and defect detection algorithm are applied. The weld extraction algorithm was developed to locate and extract welds automatically from the intensity profiles taken across the image by using graphical analysis. This algorithm was able to extract weld from a radiograph regardless of whether the intensity profile is Gaussian or otherwise. This method is an improvement compared to the previous weld extraction methods which are limited to weld image with Gaussian intensity profiles. Finally, a defect segmentation algorithm was developed to segment the defects automatically from the image using background subtraction and rank leveling method. A comparative study on weld radiograph image background estimation by rank leveling technique and polynomial surface fitting algorithm was also carried out. The rank leveling technique was found to yield better result compared to polynomial surface fitting algorithm in the tested images. The developed automated defect segmentation methodology was successfully tested on 30 weld radiographs. One main contribution of this research is the development of an automatic label removal algorithm which, to the best of the author's knowledge, no previous work has been published on this topic. The label removal algorithm developed enables the application of the defect segmentation methodology on weld radiographs which contains labels. Besides that, a weld

extraction methodology which improved the previous method was developed to extract weld area across good as well as defective welds. Finally, an automatic defect segmentation algorithm by rank leveling technique was developed to segment defective area from non-uniformly illuminated weld radiographic images. The weld extraction and defect segmentation algorithm proposed in this research are able to process noisy and non-uniformly illuminated weld radiographic images.

# CHAPTER 1

## INTRODUCTION

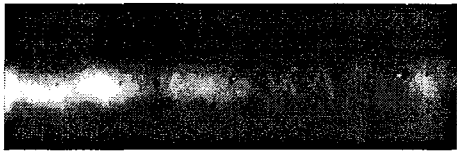
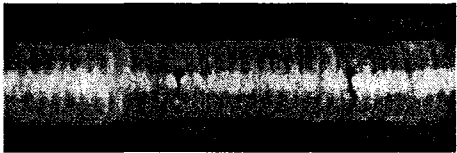
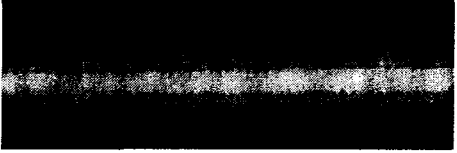
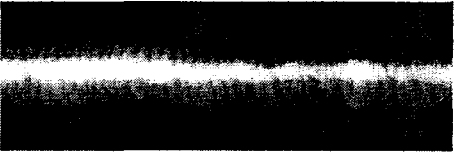
### 1.1 Background of research

Welding is a technique for joining metallic part which is usually carried out through the application of heat or pressure (Houldcroft, 1979). For critical application of weld where failure can be catastrophic, such as in pressure vessels, load-bearing structural members and power plants, welded structures often have to be tested non-destructively. Non-destructive test (NDT) is a testing method for materials and components that does not damage or destroy the test sample. Radiography testing is one of the NDT methods which are widely accepted for weld quality inspection (Hayes, 1998). Inspection of welded structures is important to ensure that the quality of the welds meets the requirements of the design standard, so that the safety and reliability of the structures can be assured.

In radiography testing, the welded structure to be examined is placed between radiation source (X-ray or Gamma ray) and the film (Hayes, 1998). The film registers the differential absorption of the radiation by the weld internal structure as a projection shadow graph. The photographic record which is recorded on the film is called a radiograph. Radiographs are generally viewed on a light box, where the quality of weld can be inspected by the trained and experienced radiographer to detect any interruptions in the typical welded structure. Interruptions that do not meet the requirements of standard, codes or specification are referred to as defects.

Several types of weld defects can be observed from a weld radiograph. The defects have various shapes, sizes, orientations and locations. The most common weld defects and their sample radiographs are presented in Table 1.1.

Table 1.1: Typical weld defects in weld radiographs  
(International Institute of Welding, 1978).

| Sample radiograph   | Weld defect details     |  |
|---|-------------------------|--|
|    | Defect                  | Porosity   |
|   | Description             | Cavities due to entrapped gas.   |
|   | Radiographic Appearance | sharply defined dark shadows of rounded contour.   |
|    | Defect                  | Slag Inclusion   |
|   | Description             | Slag or other foreign matter entrapped during welding.   |
|   | Radiographic Appearance | dark shadows of irregular contours.  |
|    | Defect                  | Incomplete Penetration   |
|   | Description             | Lack of fusion in the root of the weld or gap left by failure of the weld metal to fill the root . |
|   | Radiographic Appearance | dark continuous or intermittent line in the middle of the weld.                                    |
|   | Defect                  | Lack of Fusion   |
|   | Description             | Two dimensional defect due to Lack of union between weld metal and parent metal.                   |
|   | Radiographic Appearance | thick dark line with sharply defined edges.  |
|  | Defect                  | Crack  |
|   | Description             | Discontinuity produced by fracture in the metal.   |
|   | Radiographic Appearance | Fine dark line, straight or wondering in direction.  |
|  | Defect                  | Undercut   |
|   | Description             | a groove or channel in the surface of the plate along the weld edge.                               |
|   | Radiographic Appearance | A dark line, sometime broad and diffuse, along the edge of the weld                                |

Conventionally, a weld radiograph is checked and interpreted by a human inspector. The interpretation of radiographs takes place in three basic steps which are: detection, interpretation, and evaluation (Liao *et al.*, 2000). All of these steps make use of the radiographer's visual perception. The ability of a radiographer to detect defects in radiographs is affected by the quality of the radiograph, size of the defects, the experience level for recognizing various features in the image, etc. The result of the interpretation is very much dependent on the capability and experience of the radiographer.

The major setbacks of the interpretation of weld radiograph by human inspector are that they are very subjective, inconsistent, labor intensive, and biased (Liao & Ni, 1996). Due to the nature of image formation and resultant image quality, the radiographic image presents many problems to human inspector, which makes interpretation of weld radiographic images very difficult and inconsistent (Jagannathan *et al.*, 2000). Moreover, human inspectors require training and their skills may take time to develop. Although humans can do the job better than the machine in many cases, they are slower than the machine and get tired quickly (Malamas *et al.*, 2003).

Radiographs are normally viewed on a light-box. However, it is becoming increasingly common to digitize radiographs and view them on a high resolution monitor (Hayes, 1998). Due to the recent development in the fields of computer vision and digital image processing, automatic inspection is being widely applied in many fields such as defect analysis, detection of welding defects, part measurements, assessment of surface texture, and etc (Shafeek *et al.*, 2004).

For the past several years, few attempts have been made to develop a computer aided interpretation system for detecting defects in welds (Lawson and Parker, 1994; Bonser and Lawson, 1998; Liao *et al.*, 1999). A computer aided weld

quality interpretation system generally comprises of three major functions: weld extraction, defect segmentation and defect classification. Weld extraction refer to the operation of segmenting welds from the background. Defect segmentation on the other hand is an operation of segmenting flaws in the weld while defect classification is to classify the types of segmented flaws.

Lim (2004) developed an automatic defect classification methodology from weld radiographs by using a Multilayer Perceptron (MLP) neural network. ~~The author proposed a weld extraction and defect segmentation algorithm to segment the weld defects from the radiographic image before applying the defect classification methodology to the segmented defects. However, weld extraction algorithm proposed by author failed to extract weld from noisy images and images that contain labels. On the other hand, defect segmentation algorithm proposed by Lim (2004) also failed to perform ideally on a noisy and non-uniformly illuminated weld radiographs. In segmenting defects, it was found that some noise cluster also appeared in the binary image. More details on the weld extraction and defect segmentation algorithm proposed by author are discussed in Chapter 2. The focus of the author's research is to develop an automatic defect clarification system that is able to detect and classify multiple defects in weld radiographs. This research is a continuation of Lim's (2004) work where an automatic weld defect segmentation methodology which aims to segment weld defect from the whole section of weld radiographs was proposed. The output of the automatic weld defect segmentation methodology proposed in this research is a binary image showing the segmented defects.~~

## **1.2 Problem statement**

Before carrying out weld defect segmentation, weld extraction operation is normally carried out to extract the weld region from the entire image. However in certain weld radiographic images, labels may be included to indicate the weld number

or other identification (American bureau of Shipping, 2002). These labels need to be removed from the radiographic images in order to ensure that the weld extraction algorithm will not be affected. To the best of the author's knowledge, no research in this area has been published in the literature. The absence of an automatic weld radiograph label removal algorithm limits the application of weld extraction algorithm on a label-free weld radiographic images.

The reason for applying weld extraction algorithm before defect segmentation stage is to avoid unproductive processing of the background image and also to avoid the occurrence of false alarm from the detection of noise in the background image. To date, not much literature has been published in this area. Some of the methodologies that were proposed in previous research failed to extract weld from non-uniformly illuminated images (Gueudre *et al.*, 2000, Lim, 2004). On the other hand, methodology proposed by Liao and Ni (1996), Liao *et al.*, (2000) used intensity profile of weld radiographic images to extract weld. Their methodology is limited to images with Gaussian-like intensity profile.

In a digital radiographic system there is a variety of imaging noise, which originates from most of the elements of the system, such as charge coupled device (CCD) camera, imaging screen, radiation source, etc (Chen, 2000). Besides that, the images may be corrupted by non-uniform illumination (Lashkia, 2001). The major problems suffered by current defect segmentation algorithms are unable to segment defects from a noisy, low contrast and non-uniform illuminated radiographic images (Lashkia, 2001).

### **1.3 Research objectives**

The main objective of this research is to develop an automated weld defect segmentation methodology that can segment defects on low contrast and noisy radiographic images.

To achieve the goal of developing an automated weld defect segmentation methodology, three sub objectives of the research have been identified, including:

- (a) To develop an automatic label removal algorithm in order to remove labels printed on the weld radiographic images.
- (b) To develop an automatic weld extraction algorithm so that weld region in the image can be segmented from the background image.
- (c) To develop a defect segmentation algorithm capable of segmenting multiple defects that occurs in welds from a single radiograph image.

### **1.4 Research Scopes**

The developed automated weld defect segmentation methodology serves as a pre-processing stage for defect classification methodology. Defect classification

methodology was developed earlier by Lim (2004) and therefore is not included in this research.

The scopes of this research are:

- ~~Welding for the metals is not included in the scope of this research.~~
- ~~Radiography testing on weldment is not included in the scope of this research.~~
- Weld radiographs are provided by Malaysia Institute of Nuclear Technology (MINT).
- Digitization of weld radiograph by using a high resolution digital scanner was carried out at MINT.
- The entire algorithm and computer program are written by using Matlab programming language.

## **1.5 Research Approach**

First of all, literature review on automatic weld radiograph inspection was carried out. Automatic weld extraction and defect segmentation were two major focus topics. Past research on these two topics are reviewed thoroughly to determine the current state-of-art in this research.

In order to carry out the weld extraction process more effectively, an algorithm was developed to remove labels from the weld radiographic images. The existence of label pixels in an image was confirmed with a normality test. Any detected label pixels were removed from the image with a series of image processing techniques. The algorithm was tested on radiograph image with labels which contains various types of weld defects to prove its effectiveness. The algorithm was also tested on label-free

radiographic images to show that the proposed algorithm does not remove any other details from the image except the labels. The label removal algorithm removes labels from the radiograph and the label free image was then subjected to the weld extraction process.

An automatic weld extraction algorithm based on image intensity profile was developed. The weld boundary was determined by using graphical analysis of weld intensity profile taken across the image. Boundary point detection of weld region was carried out on every intensity profiles taken across the weld area. Finally, the weld boundary points were connected to form weld upper boundary and weld lower boundary. As a result, the weld region which is located between weld upper and lower boundaries was extracted.

Finally, an automatic defect segmentation algorithm was developed. This algorithm only operates in the extracted weld region to speed up the processing time and also avoid unnecessarily processing in the background region. The background subtraction method was used to level the non-uniform illuminated background of the image. This was followed by contrast enhancement of the leveled image, before defect segmentation is carried out by using histogram thresholding method. Lastly, post-processing of the segmented binary image was carried out to remove false detection and noise in the image, so that only the defects remain at the end of the process.

## **1.6 Thesis outline**

This thesis is arranged in accordance to the objectives and approach as mentioned above. Chapter 2 presents the basic concept of welding process and also nondestructive testing of welded structure, which is mainly focused on radiography testing. Reviews on related research from the early stage until recent years on automatic weld extraction and defect detection will also be presented. Advantages and

limitations of the existing approaches on these two areas of interest will be discussed in detail.

Chapter 3 discusses the development of an automatic labels removal methodology to remove labels printed on weld radiographic images. Chapter 4 presents an automatic weld extraction methodology based on gray level profiles of the weld radiograph to segment the weld region from the background.

In chapter 5, automatic defect segmentation methodology on extracted weld region by background subtraction method using rank leveling technique has been proposed. Comparative study of background subtraction method by using rank leveling and surface fitting algorithm has also been carried out. Chapter 6 discusses the integration of the label removal algorithm, weld extraction algorithm and also defect segmentation algorithm which were developed in Chapter 3, Chapter 4 and Chapter 5 respectively. Integration of these algorithms provides a fully automated weld defect segmentation methodology which is able to segment the weld defect from digitized weld radiographic images.

Finally, conclusions of this research are drawn in Chapter 7. Recommendations and suggestions for future research are also provided.

## **CHAPTER 2**

### **LITERATURE REVIEW**

#### **2.1 Introduction**

This chapter presents an overview of welding process and also non-destructive testing of weld, which is mainly focused on radiography testing. Concept of welding process and classification of welding types are briefly discussed. After that, basic theory of weld structure non-destructive testing, especially radiography testing is presented. Next, literature review on automatic weld radiograph inspection is carried out. Special attention is focused on three major topics, which are automatic label removal, automatic weld area extraction and also automatic defect segmentation of weld radiograph. Recent studies and researches on these areas are reviewed thoroughly, where advantages and limitations of past researches are identified to determine the area that need to be focused in this research.

#### **2.2 Overview of welding process**

Welding is a process of joining together two pieces of metal, which uses heat or pressure or both, and with or without added metal (Houldcroft, 1979). Welding process can be classified into two major categories: fusion welding and non-fusion welding (solid state welding). Fusion welding is any process of joining metals that involve the melting of parent metals. On the other hand, non-fusion welding or solid state welding is the process of joining metals that does not involve the process of melting the parent metals. Figure 2.1 illustrates a classification of the welding processes.

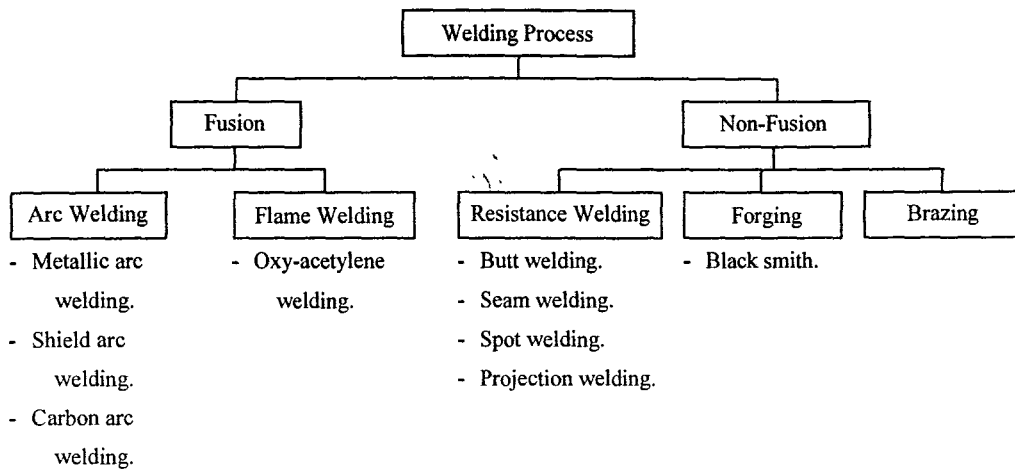


Figure 2.1: Classification of welding processes.

Two main processes in fusion welding are arc welding and flame welding. Arc welding use the heat created by an electric current to raise the temperature of parent metals to the appropriated welding temperature. Examples of arc welding are metallic arc welding, shielded arc welding and carbon arc welding. Flame welding on the other hand uses heat from ignited gases to melt the parent metal. Flame welding is usually done with oxy-acetylene flame, although other mixtures of fuel gas and oxygen are sometimes used (Pender, 1968).

There are three main types of non-fusion welding: forging, resistance welding and braze welding. In forging process, metals will be heated to the correct temperature in a fire. The parts are then hammered and joined together by the pressure of hammering. In resistance welding, the parts to be welded are clamped between two electrodes. The heat is then generated by an electric current and flows through the electrodes and the welding will be formed between metals on the contact point of the electrodes. For braze welding process, a welding rod is required to join two metals

together. The parent metals are heated to a temperature which is lower than its own melting point, but higher than the melting point of the welding rod. Therefore, pieces of metal will be joined by the molten metal from the welding rod.

Arc welding is a joining process that is widely used today (Pender, 1968). It is a fusion process because it melts the base metals being joined. As the electrode is brought close to the base metal, an arc is created by an electric current that flows between the electrode and the base metal. The arc causes the base metal and the electrode to melt and the molten metal from the electrode then flows into the joint. Three distinct zones can be identified in a typical arc welding joint (as shown in Figure 2.2): base metal, heat-affected zone and weld metal (Kalpakjian and Schmid, 2001).

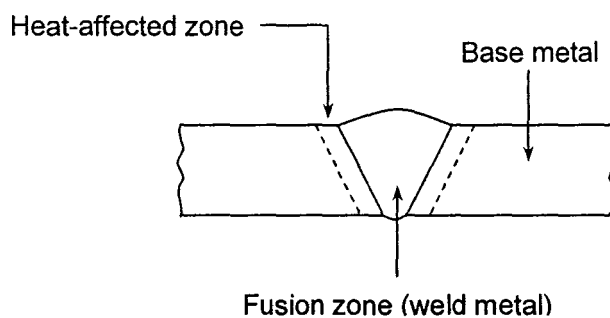


Figure 2.2: Three distinct zones of a typical arc welding joint.

### **2.3 Non-destructive testing of welded structure**

Weld structure always has to be tested non-destructively to examine the quality of the welds (Liao and Ni, 1996). Non-destructive test (NDT) are examinations carried out on the component, which do not damage the component, and after successfully testing, the component may be put into service. The most common types of NDT for weld structures are: ultrasonic testing, radiographic testing, magnetic particle testing and liquid penetrant testing (Haynes, 1987).

In ultrasonic testing, high frequency sound beam is directed through the weld. When the sound beam strike an interruption in the material continuity (weld defects), some of the sound will be reflected back and collected by an instrument and displayed on a screen. In radiographic testing, gamma or X-ray is transmitted from the radiation source through the weld structure and onto a film. Weld internal features are indicated as lighter and darker areas on the film. Magnetic particle testing on the other hand is a method of locating defects in magnetic materials. When a component is magnetized; any defects will make leakage fields and attract magnetic particles. Liquid penetrant testing is widely use for leakage detection. A common procedure is to apply fluorescent material to one side of the joint and view the other side with ultra violet light to check for any leakages (Hayes, 1998).

Radiographic testing is one of the most important, versatile and widely accepted NDT methods for weld quality inspection (Hayes, 1998). Radiographic testing involves the use of penetrating gamma or X-radiation to examine product's defects and internal features. X-rays are produced by high-voltage generators while gamma rays are produced by the atomic disintegration of radioisotopes. An X-ray machine or radioactive isotope is used as a source of radiation and the radiation produced is directed through a weld and onto film. The resulting radiograph shows the internal features and reliability of the weld. Material thickness and density changes are

indicated as lighter or darker areas on the film. When less absorption of the radiation energy happens due to the thin section or low density of the metal, dark region occurs in the radiograph. On the other hand, thicker or higher density area absorbs more radiation energy and therefore the corresponding area on the radiograph will appear lighter. Figure 2.3 illustrates the working principle of radiographic testing of weld.

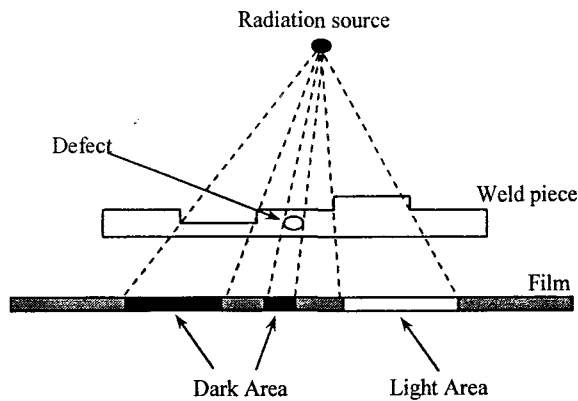


Figure 2.3: Radiographic testing.

## 2.4 Application of machine vision on weld inspection

Industrial radiography is a traditional technique for evaluating welded structure quality. Digital image processing techniques allow the interpretation of the radiographic images to be automated. Avoiding the presence of human inspectors makes the inspection system more reliable, reproducible and faster. Moreover, the high level image processing methods can even replace the expert's knowledge (Jagannathan *et al.*, 2000).

Automated X-ray inspection has been an active field of research for the past several years (Shashishekhar, 2004). Preprocessing process prepares the acquired raw digital images for defect segmentation stage by reducing noise, contrast

enhancement and removing geometric structures which otherwise would affect the defect segmentation stage. In automated weld radiograph inspection, this normally involves welds extraction. Lawson and Parker (1994), Gueudre *et al.* (2000), Liao and Ni (1996), Liao *et al.* (2000) and Lim (2004) were among the researchers who has been working on the topic of automated weld extraction.

Defects are characterized in radiographic images by local discontinuities in the intensity values of the image. The defect segmentation process can be considered as pixel classification problem, where the aim is to classify each image pixels as defect or non-defect (Shashishekhar, 2004). Methods which were applied by previous researchers in automatic defect segmentation are background subtraction (Wang and Liao, 2002; Lim 2004), template matching (Bonser and Lawson, 1998), intensity profile analysis (Liao and Li, 1998; Just *et al.*, 1998), artificial neural network (Lawson and Parker, 1994; Jacobsen and Zscherpel, 1999; Nafaa *et al.*, 2000), fuzzy logic (Liao *et al.*, 1999; Lashkia, 2001; Kaftadjian *et al.*, 2003) and adaptive thresholding (Kehoe *et al.*, 1989; Palenchika and Alekseichuk, 1999).

In defect classification stage, the defect pixels identified from the previous stage are group into connected regions, their characteristics were measured, classified into different types, and finally accept or reject decision was made based on the inspection criteria.

## **2.5 Label removal from weld radiographs**

To the best of the author's knowledge, there is no work published on the research area of automatic label removal from weld radiographs. The most relevant work, however, was mentioned in automatic weld extraction methodology published by Lawson and Parker (1994), and Liao and Ni (1996).

Lawson and Parker (1994) ignored labels in the image during the training of the neural network for weld extraction. After training, the network was applied to the weld radiograph with labels and the segmentation result shows that weld region was successfully extracted and the labels in the image were ignored. Liao and Ni (1996) used intensity profile analysis method for weld extraction. Peaks were observed on an intensity profile when it was taken across label and weld region. They developed an algorithm to identify and extract the peak which is associated to the weld area. By this, peaks which belong to labels in the image were neglected.

Both methodologies discussed above did not remove the labels from the image. Instead of that, these methodologies were somehow trying to “avoid” label in the image when performing the weld extraction process. However, it is preferable to remove labels from the image entirely in order to make sure weld extraction and defect segmentation processes which is to be performed after will not be affected by labels in the image. Besides that, removal of labels from the image also can avoid the false alarm from occurring during the defect segmentation stage, where the labels would be segmented as defects.

In this research, a label removal algorithm was developed to remove the labels from weld radiographic images before weld extraction and defect segmentation algorithm is applied.

## **2.6 Weld extraction in weld radiographs**

The extraction of weld from the background is very important to avoid unproductive processing of the background image during defect detection process. By reducing the unproductive processing of image data, the processing time can thus be reduced. Weld extraction also aims to avoid the occurrence of false alarm due to the detection of noise and intensity variation in the background region.

Lawson and Parker (1994) developed a Multilayer Perceptron (MLP) neural network to extract the weld region from weld radiographs. The image was first filtered with a  $5 \times 5$  low pass filter to reduce noise in the image. After that, the network was trained with a single image showing a typical weld that is to be inspected, coupled with a very simple schematic weld "template", as shown in Figure 2.4(a) – 2.4(c). Their neural network was proven to be able to extract the weld region after a lengthy training period (40,000 training samples). However, their algorithm used smoothing operators, which were very poor in performance for detecting small defects. When these operators were used, small and low contrast objects became blurred or even disappeared. Besides that, the application of only one image as a template to train the network limits the network to operate correctly only on images with similar image properties to the trained data (Lim, 2004).

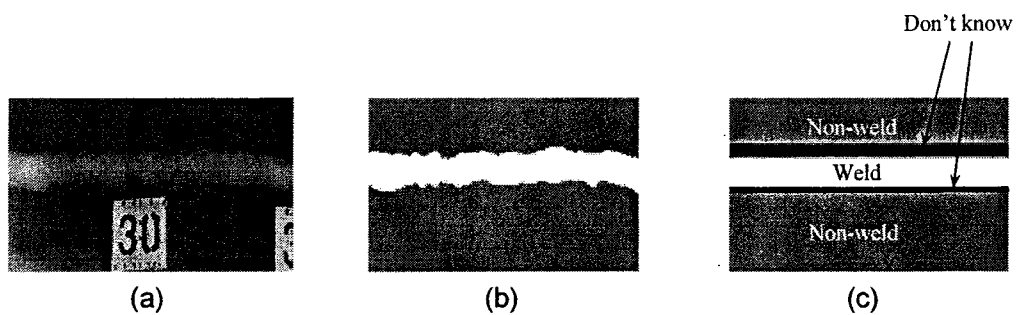


Figure 2.4: (a) Typical radiographic image (b) image from manual interpretation of the weld (c) template image used to train neural network.

Gueudre *et al.* (2000) used a fundamental image processing technique to segment the weld region based on the intensity difference between weld region and its background. By introducing the co-operative method of edge and area approach, namely 'Edge and Area Segmentation Method', the authors were able to detect the weld area in X-ray radiographic images of weld. B-spline curve method was used to carry out the segmentation of the detected weld area. However, edge detection

technique is very sensitive to noise in the low contrast images, and conventional image segmentation method is unable to properly segment non-uniformly illuminated images. That is why this method is not suitable for processing the non-uniformly illuminated and low contrast images.

Lim (2004) developed a weld extraction algorithm that is based on the intensity profile taken across the weld region. Pixels with low intensity value were regarded belong to the non-weld area in the image. These pixels were identified and used to draw a least square straight line that acted as an estimated background for the profile. Finally, location where the difference of the pixel intensity value and the estimated background straight line achieved certain threshold value was extracted as weld boundary location. However, the limitation of this method is that the intensity of non-weld area in the images must be smoothly distributed. Error was recorded when the intensity of non-weld area in the image is not smoothly distributed, especially in non-uniformly illuminated weld radiographic images.

Another weld extraction method based on the intensity profile of the weld radiographs was proposed by Liao and Ni (1996). The author's methodology was based on the observation that the intensity plot of the weld looks more like Gaussian than the other objects in the image. The algorithm developed processed the image line by line to detect the peak in the gray level profile. Peak in the line image, which fulfills certain pre-defined characteristics, was judged as weld.

As a continuation of their previous efforts on weld extraction (Liao and Ni, 1996), Liao *et al.* (2000) developed another method of weld extraction: implementation of fuzzy classifier (K-nearest neighbor (KNN) and c-means) to extract the weld region. The procedure for this method consists of three major components: features extraction, pattern classification and post-processing. For each peak in the intensity profile

extracted from the whole image, 3 features were defined: (i) width, (ii) mean square error (MSE) between an object and its Gaussian intensity plot and (iii) the peak intensity. The fuzzy KNN and fuzzy c-means algorithm were used as a pattern classifier to identify each peak as weld or non-weld. The post-processing operation was applied to remove noise generated due to false alarm, and to connect discontinues weld line due to misclassification. This method is proven able to extract linear and curved weld. However, fuzzy KNN classifier generated false alarm rate from 16.08% to 23.14% while fuzzy c-means classifier generated false alarm rate from 55.48% to 80.4%. Even after post-processing, the false alarm rate of 10.73% to 28.34% was recorded.

A major limitation of weld extraction methodology based on the Gaussian characteristic of the intensity profile of weld radiograph is that the method is limited to weld radiographs having Gaussian-like intensity profiles across the weld, as shown in Figure 2.5(a). Gaussian-like intensity profile is referring to the profile that resembles the bell shape of a Gaussian profile. Due to this reason, high false alarm rate was recorded when the methodology is tested on weld radiograph with non-Gaussian profiles (Liao and Li, 1998). Intensity profile taken across a repaired weld and the defective area of a weld radiographs usually have non-Gaussian characteristic intensity profile, as shown in Figure 2.5(b).

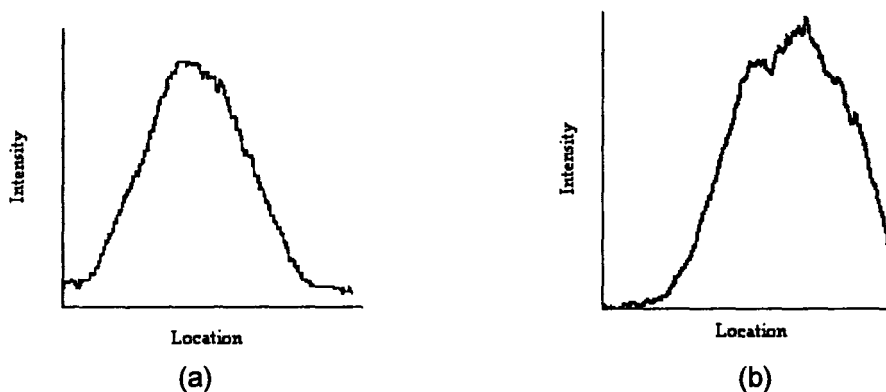


Figure 2.5: (a) Gaussian-like intensity profile (b) non-Gaussian intensity profile.

In this research, a weld extraction methodology based on the intensity profile taken across the weld area of the image is proposed. This methodology will overcome the drawbacks of current weld extraction methodology that unable to properly extract the weld region from non-uniformly illuminated images and only limited to the weld radiograph images with Gaussian-like intensity profile.

## **2.7 Defect segmentation in weld radiographic images**

One of the techniques which was applied by researchers in automatic weld defect segmentation is background subtraction method. In background subtraction method, the background image was estimated from the original image. The estimated background image was then subtracted from the original image and the suspected defects were detected (Russ, 1999).

Wang and Liao (2002) estimated the background model of weld radiographic image by surface fitting algorithm based on a polynomial function. The weld image was converted into a format of three dimensional data, which indicated the location of the pixel in x-axis, y-axis and the intensity value of the pixel. This data was then imported into Statistical Package for the Social Sciences (SPSS) software and the image background model was constructed based on a second order polynomial function. After the background was subtracted from the image, histogram thresholding was carried out to eliminate noise pixels and thus, defects in the image can be segmented. However, it is very difficult to estimate an irregular background image by a simple polynomial function (Russ, 1999).

Lim (2004) proposed another defect segmentation methodology by using background subtraction and adaptive thresholding technique. The background subtraction method proposed by him is almost similar to Wang and Liao (2002)

method, where a polynomial surface fitting algorithm was used to obtain the background image. Weld radiographic image was divided into 30 rows and 100 columns sub-regions and pixel with highest intensity value in each sub-region was selected to obtain the estimated background image using the second order polynomial function. After background subtraction, adaptive thresholding operation was carried out on the subtracted image. The result shows that there are many noise clusters in the image after thresholding, especially for a non-uniformly illuminated background images. This is due to the reason that it is very difficult to estimate an irregular background image by a simple polynomial function (Russ, 1999).

Besides background subtraction method, intensity profile analysis was another technique which has been explored. Liao and Li (1998) suggested that intensity profile taken across a flawless weld has a Gaussian-like bell shape and welding flaws will distort this bell shape of the intensity profile. Spline curve fitting was applied to smooth the intensity profiles and reduce the noises. This was followed by a profile anomaly detection algorithm to identify abnormalities on the bell shape of the profile. Anomaly detection algorithm searches for 3 types of profile anomalies, namely peak-anomaly, trough-anomaly and slant-concave-anomaly, as shown in Figure 2.6(a) - 2.6(c).

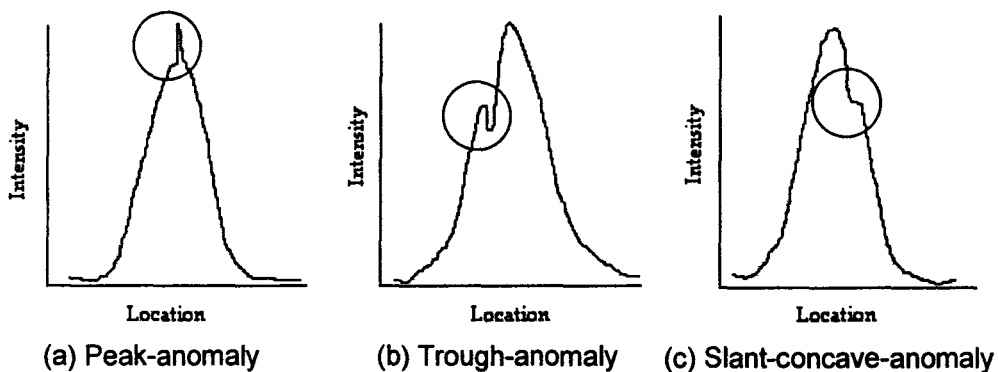


Figure 2.6: Weld radiographic image profile anomalies.

A 2-dimensional flaw-map was then generated for every processed intensity profile. However, this methodology is unable to process welds with non-Gaussian intensity profiles. High false alarm rate on non-Gaussian intensity profile is expected since the methodology was developed based on Gaussian characteristics of intensity profile. Besides that, 2-dimensional flaw map generated does not show actual shape and geometry of the detected defects.

Another intensity profile analysis algorithm was developed by Just *et al.* (1998) to detect crack-like defects in the weld radiograph images. From the intensity profile taken across weld, a pre-set contrast-based criterion was used to differentiate defects from noises in the image. However, this algorithm is only limited to the detection of crack-like defects.

Adaptive thresholding is another segmentation technique which was applied by other researchers in automatic weld defect detection. Adaptive thresholding is a segmentation method where the threshold value will change over the image according to the local image characteristics. Kehoe *et al.* (1989) applied defect detection with a newly developed adaptive edge detection operator, namely mean gradient edge detector (MGED). A window is scanned over the weld radiographs where the mean and gradient value of the window is determined. Based on the mean and gradient value, center pixel of that window is classified as defect or non-defect. The main disadvantages of this method are large amount of processing required to complete edge detection and edge detection techniques are also very sensitive to noises in the image (Lashkia, 2001).

Palenchika and Alekseichuk (1999) proposed another method for automatic defect detection in weld radiographic images by using structure-adaptive binary segmentation. Weld radiographic image background and defects were approximated

by a polynomial model. Features based on object shapes and intensity attributes were used to locate the defects. The drawback for this type of model based approach is that it is only limited to certain type of defects (Kaftandjian *et al.*, 2003).

Bonser and Lawson (1998) proposed a template matching defect enhancement technique for automatic defect detection in weld radiographs. They used Laws filter (Figure 2.7(a)) matched for round defects, and Kirsch filter (Figure 2.7(b)) for longitudinal defects. After the defects were enhanced, defect segmentation was carried out based on the value of standard deviation of local area population. The standard deviation value was thresholded to detect areas of high variance (likely to be defects) and low variance (likely to be background). However, template matching approach required 'a priori' knowledge in order to match the predefined filters to different kind of defects. They also concluded that filtering approach is less sensitive to small defects.

|    |   |    |   |    |
|----|---|----|---|----|
| -1 | 0 | 2  | 0 | -1 |
| -2 | 0 | 4  | 0 | -2 |
| 0  | 0 | 0  | 0 | 0  |
| 2  | 0 | -4 | 0 | 2  |
| 1  | 0 | -2 | 0 | 1  |

(a) Laws filter

|    |    |    |    |    |
|----|----|----|----|----|
| 1  | 1  | 1  | 1  | 1  |
| 1  | 1  | 1  | 1  | 1  |
| 0  | 0  | 0  | 0  | 0  |
| -1 | -1 | -1 | -1 | -1 |
| -1 | -1 | -1 | -1 | -1 |

(b) Kirsch filter

Figure 2.7: Filter masks for defect detection.

Application of artificial intelligence (AI) techniques such as artificial neural network (ANN) and fuzzy logic, on automatic defect detection of weld radiographic images have also been explored. Lawson and Parker (1994) trained a MLP neural network based on Kehoe's (1989) adaptive threshold operator. The trained network scans the image in a raster fashion, where the input of the network was corresponded to a window of size  $m \times n$ . The center pixel of the window was classified into

background and defect accordingly. They compared their neural networks with the original Kehoe's adaptive threshold and found that their neural networks perform better in defect segmentation compared to the original Kehoe's adaptive thresholding method.

Jacobsen and Zscherpel (1999) proposed a method to detect crack and undercut type of defects in the weld radiographs based on ANN. The features were extracted from the intensity profile using various types of filters, namely morphological filter, Derivative of Gaussian filter, Gaussian Weighted Image Moment Vector Operator (GWIMV) filter, Fast Fourier Transform (FFT) filter and Wavelet transform filter. Extracted features were used as an input to a neural network to identify the intensity variations of the profile. The major setback of this work is the limitation of the network to detect crack and undercut defects.

Nafaa *et al.* (2000) applied an ANN for edge detection of weld defects in radiographic images. To extract the edges of the weld defect, a  $3 \times 3$  window slides over the entire image and the network classifies each center pixels of the window as edge or non-edge based on the intensity value of its neighboring pixels. Thus, the network has nine neurons receiving the intensity value of pixels composing the  $3 \times 3$  window. The output layer contains one neuron which classifies the center pixel of the window as edge or non-edge, as shown in Figure 2.8(a). 28 training couples of input and output were chosen based on the most dominant contour cases, as shown in Figure 2.8(b). However, the edge detection method is very sensitive to noise in the image.